

Invited Paper

**MORE DETAIL VIEW ON THE DYNAMICS
OF THE IMPACT DAMPER***UDC 534.014:534.1:681.34***Peterka František**

Institute of Thermomechanics, Academy of Sciences of the Czech Republic
Dolejškova 5, 182 00 Prague 8, Czech Republic, E-mail: peterka@it.cas.cz

Abstract. *The motion of the dynamical impact damper is studied using numerical simulation. Regions of existence and stability of different regimes of the system response on the harmonic excitation is evaluated. Boundaries of regions are specified as grazing, period doubling, saddle-node and Hopf bifurcations. Periodic, quasiperiodic and chaotic impact motions are explained by time series, phase trajectories, bifurcation diagrams and Poincarè maps.*

1. INTRODUCTION

The dynamics of impact dampers was extensively examined theoretically and using analogue computer simulation approximately forty years ago (see e.g. [1-27]). Their principle consists in the supplement of a small mass, which can decrease of resonance amplitudes of vibrating system due to mutually impact interactions. There were several constructions the mechanical models are shown in Fig. 1. The logical series of impact dampers (Fig. 2), which express the transition between classical tuned absorber (Fig. 2(a)) and usual impact damper (Fig. 2(d)) was studied in [6]. Impact dampers parameters were optimised from the point of view of flat amplitude characteristics in the neighborhood of the original system resonance [7].

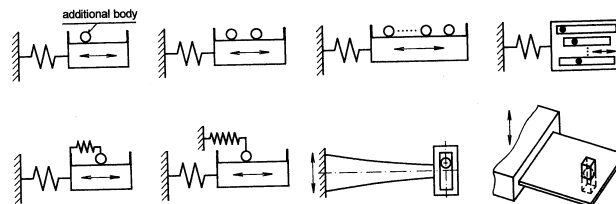


Fig. 1. Examples of impact dampers

Later were investigated in more detail, especially by numerical simulation, problems of the influence of dry friction on the impact dampers dynamics [8], bifurcations and chaos [9, 10].

This paper describes the behavior of dynamical impact damper (Fig. 2 (c)).

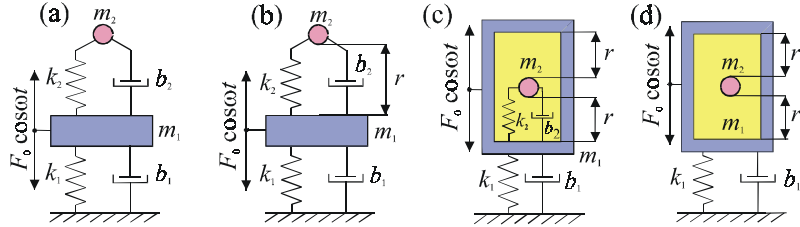


Fig. 2. Schemes of linear-tuned damper (a) and impact dampers (b) - (d)

1. MATHEMATICAL MODEL OF THE DYNAMICAL IMPACT DAMPER

The damper (Fig. 3) consists from a main mass m_1 , which is periodically excited and its resonance amplitudes should be minimised by the influence of the additional mass m_2 motion. The additional mass moves in the longitudinal cavity of the main mass and it can impact on one or both obstacles. Masses are connected by a linear spring k_2 and a linear damper b_2 . The fundamental motion of this impact damper was solved theoretically including the influence of the dry friction in [11].

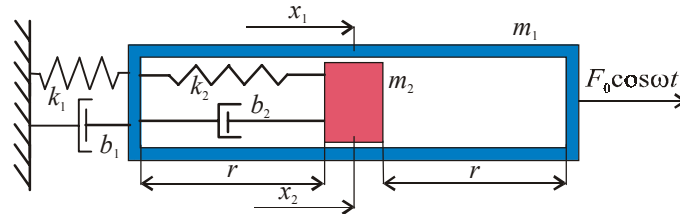


Fig. 3. Scheme of the dynamical impact damper

The motion of the assumed damper is described by equations

$$m_1 \ddot{x}_1 + b_1 \dot{x}_1 + k_1 x_1 + b_2 (\dot{x}_1 - \dot{x}_2) + k_2 (x_1 - x_2) = F_0 \cos \omega t, \quad (1)$$

$$m_2 \ddot{x}_2 - b_2 (\dot{x}_1 - \dot{x}_2) - k_2 (x_1 - x_2) = 0. \quad (2)$$

They can be written in the form

$$X_1'' + 2bX_1' + 2\beta b(X_1' - X_2') + \mu \varepsilon^2 (X_1 - X_2) = \cos \eta \tau, \quad (3)$$

$$X_2'' - 2(\beta b / \mu)(X_1' - X_2') - \varepsilon^2 (X_1 - X_2) = 0, \quad (4)$$

after the amplitude transformation $X = x / x_{1st}$, ($\rho = r / x_{1st}$) and time transformation $\tau = \Omega_1 t$,

where $x_{1st} = F_0/k_1$; $\Omega_1 = \sqrt{k_1/m_1}$; $b = b_1/(2\sqrt{k_1m_1})$; $\beta = b_2/b_1$; $\mu = m_2/m_1$;
 $\varepsilon = \Omega_2/\Omega_1$; $\Omega_2 = \sqrt{k_2/m_2}$; $\eta = \omega/\Omega_1$.

Equations (3), (4) determine the numerical simulation of the impactless motion. When the relative motion of masses m_1, m_2 meets the condition of impact

$$|X_1 - X_2| \geq \rho, \quad (5)$$

then velocities of masses will change suddenly according to equations resulting from the Newton theory of direct and centric impacts:

$$\begin{aligned} X'_{1+} &= X'_p - X'_{rel-} R m_2 / (m_1 + m_2), \\ X'_{2+} &= X'_p + X'_{rel-} R m_1 / (m_1 + m_2), \end{aligned} \quad (4)$$

where $X'_p = (m_1 X'_{1-} + m_2 X'_{2-}) / (m_1 + m_2)$ is the velocity of masses after plastic impacts, X'_{1-}, X'_{2-} are before-impact velocities, X'_{1+}, X'_{2+} are after-impact velocities, $X'_{rel-} = X'_{1-} - X'_{2-}$ and $0 \leq R \leq 1$ is the coefficient of restitution ($R = 0$ and $R = 1$ for absolutely plastic and elastic impacts, resp.).

3. REGIONS OF EXISTENCE OF DIFFERENT REGIMES OF IMPACT MOTION

A more general view of the system response in the dependence on dimensionless excitation frequency η and dimensionless clearance ρ is offered by the evaluation of the existence and stability regions of different periodic and chaotic motions (Fig. 4). Regions were ascertained by quasistatic changes of parameters η, ρ . Regions are labeled by quantity $z=p/n$, where p is the number of impacts and n is the number of excitation period T in the impact motion period. Quantity z of the chaotic motion can be ascertained from the sum of impacts appeared during long time interval (e.g. thousand of periods T). Fundamental motions are characterised by $n=1$, e.g. $z=0/1, 1/1, 2/1$ (see Figs. 5, 6, 7).

Regions are surrounded by boundaries, which are labeled in correspondence with the type of the bifurcation appeared on it.

The basic boundaries marked g_z correspond to *grazing bifurcation*, which is characterized by the appearance of a new impact in the motion period when motion trajectory begins touch the stop. Grazing boundary $g_{0/1}$ in plane η, ρ expresses the amplitude-frequency characteristic of relative impactless motion $|X_1 - X_2|$. The grazing boundary represents the impenetrability condition of moving bodies and it is stronger than the stability condition. It means, that a certain periodic system motion can be theoretically stable, but it cannot physically exist, when it does not meet the impenetrability condition.

Other boundaries represent different kinds of the motion instability. Boundaries marked PD_z and Q_z correspond to the continuous transition from one periodic impact motion into another motion through the Hopf bifurcation. Important is the reversible quasistationary transition cross these boundaries. The periodic impact motion splits on stability boundaries PD_z . The Feigenbaum cascade of splitting can terminate in the

chaotic motion, but the transition from periodic to chaotic regimes with impacts is manifold [12].

Quasiperiodic motion appears on boundaries Q_z . Phase trajectories, Poincaré maps and time series of quasiperiodic $z = 2/1$ motion are shown as an example, in Figs. 10 (a), (b), (c), which correspond to point $P4$ in Fig. 4. Boundaries PD_z and Q_z open beat motion regions, in which exist quasiperiodic and periodic subharmonic motions as well as chaotic impact motions. Their period n or quasiperiod is higher than one, see for example $n = 3, 7, 73.5867$ and Figs. 8, 9, 10(c), respectively.

Topological map of impact motions in beat motion regions is very complex. The biggest region exists near the second resonance of impactless motion ($\eta=1.28$) in frequency interval $0.95 < \eta < 1.8$. The largest subregion of periodic subharmonic $z = 2/3$ impact motion with point $P2$ is shown in Fig. 4. The complexity of motions in beat motion region is better shown in Fig. 12, where bifurcation diagrams were recorded along section a in interval $1.1 < \eta < 1.63$ in Fig. 4. Subharmonic and chaotic motions exhibit hysteresis phenomena, i.e. the system response is ambiguous. Even two different chaotic motions for the same system parameters were ascertained. They differ by the extent of amplitudes and impact velocities. For example, both weak chaos (Figs. 11 (a), (b)) and strong chaos (Figs. 11 (c), (d)) exists in point $P5$ in Fig. 4.

Remaining boundaries are labeled by SN_z and SN_{CH} . They express saddle-node bifurcation of periodic or chaotic impact motions, respectively. They are characterised by the nonreversible jump transition from one stationary motion into another one. The saddle-node bifurcation is generalised also on chaotic motion, because boundaries SN_{CH} have quasideterministic shape, but their evaluation is more difficult.

Grazing and saddle-node bifurcation boundaries create hysteresis regions, where the system response is ambiguous. The biggest hysteresis region exists between boundaries $g_{0/1}$ and SN_{CH} over the second resonance $\eta = 1.28$, where either impactless motion $z = 0/1$ or beat motion $z = (0 \div 2)/1$ can exist. Another example of hysteresis region between regions of fundamental motions $z = 2/1$ and $z = 4/1$ is bounded by boundaries $g_{2/1}$ and $SN_{4/1}$ in frequency interval $0.6 < \eta < 1.2$ for low clearances ρ . The transition beat motion region between regions of $z = 2/1$ and $z = 4/1$, bounded by boundaries $PD_{2/1}$ and $PD_{4/1}$, exists in frequency interval $1.2 < \eta < 1.8$ in Fig.4.

The quantity z increases when clearance ρ approaches to zero. The system becomes one degree of freedom system with joined masses m_1 and m_2 .

4. MORE DETAIL EXPLANATION OF IMPACT DAMPER DYNAMICS

4.1 Existence of asymmetric regimes of impact motions

In spite of the symmetry of static position of mass m_2 relative to obstacles of mass m_1 , there exist many asymmetric periodic motions of the impact damper. The reason of this phenomenon will be explained using the fundamental $z=2/1$ motion (Fig. 7(a)). Its phase trajectory is centrally symmetric. When the periodic symmetric $z=2/1$ motion loses its stability on the Hopf bifurcation boundary (see point A in Fig. 15), then appears either new stable, but asymmetric, $z=2/1$ motion (see development of system motion from unstable point A_1 into fixed points B, C in Fig. 15 and phase trajectory in Fig. 7(b)), or

quasiperiodic limit cycle $z=2/1$ (see development of system motion from unstable point A_2 into limit cycle D in Fig. 15 and Fig. 13).

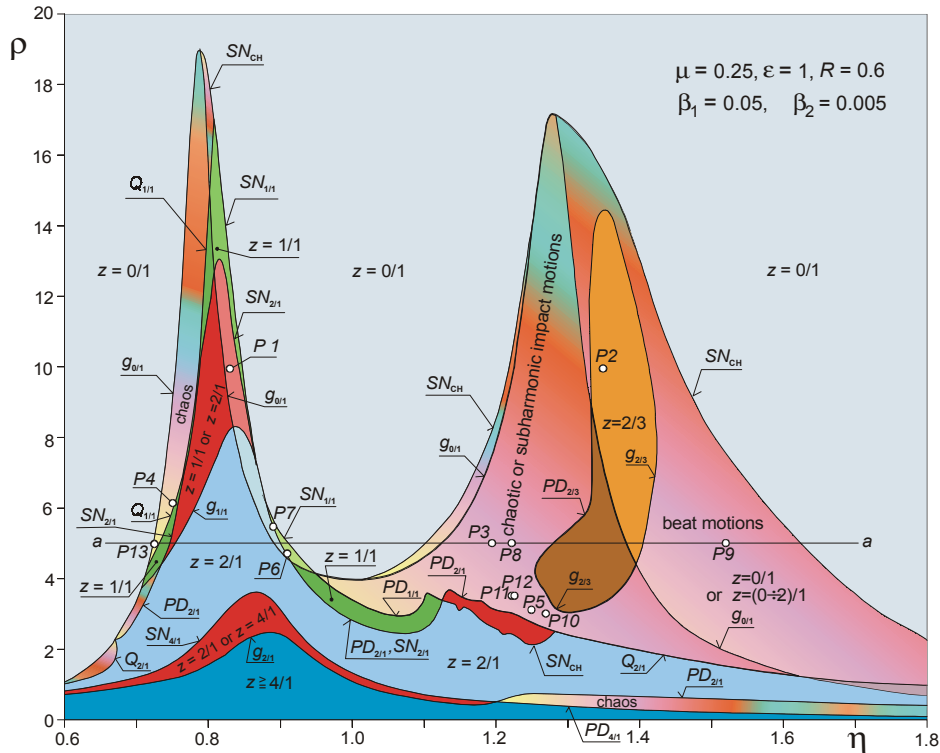


Fig. 4. Regions of existence and stability of impact motions

The asymmetric $z=2/1$ motion (Fig. 7(b)) can be assumed as the result of period doubling of unstable periodic motion $z=1/(1/2)$ in one half period of symmetric motion $z=2/1$ (Fig. 7(a)). It is the reason why bifurcation boundaries of regions $z=2/1$ in Fig. 4 were named $PD_{2/1}$, even though the period of $z=2/1$ motion remains the same and the instability indicates by the transition from symmetric into asymmetric $z=2/1$ motion.

The asymmetry of impact motion appears also in other periodic, quasiperiodic and chaotic motions. Asymmetric periodic motions can be subjected, similar as other periodic motions to grazing, Hopf's or saddle-node bifurcation. For example the asymmetric $z=2/1$ impact motion (Fig. 7(b)) can jump into periodic $z=1/1$ motion (Fig. 6(a)) on its saddle-node stability boundary. The existence of $z=1/1$ motion can be developed therefore from the symmetric $z=2/1$ motion (Fig. 7(a)) through the sequence of the Hopf and saddle-node bifurcation. It follows from Figs. 5-7(a), that there exist four different response of the impact damper for the same system parameters corresponding to point $P1$ in Fig. 4: impactless motion (Fig. 5), $z=1/1$ motion (Fig. 6(a), (b)) and its mirror regime (Fig. 6(c), (d)) and $z=2/1$ motion (Fig. 7(a)). It is expressed also by the fact, that point $P1$ in Fig. 4 belongs as the hysteresis region ($z=1/1$ or $z=2/1$) as the hysteresis region between boundaries $g_{0/1}$ and $SN_{1/1}$.

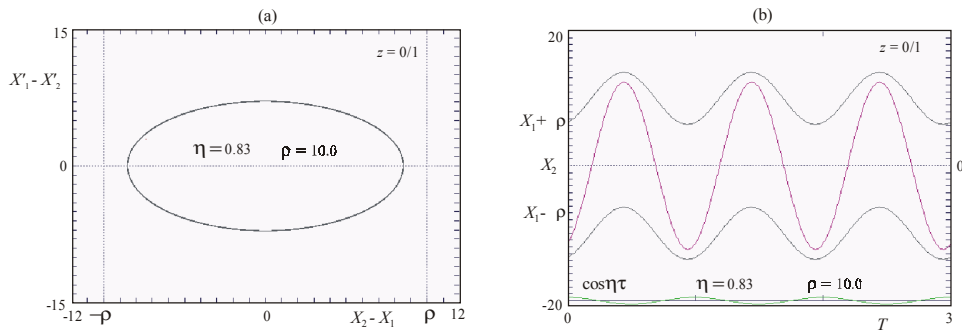


Fig. 5. Impactless motion

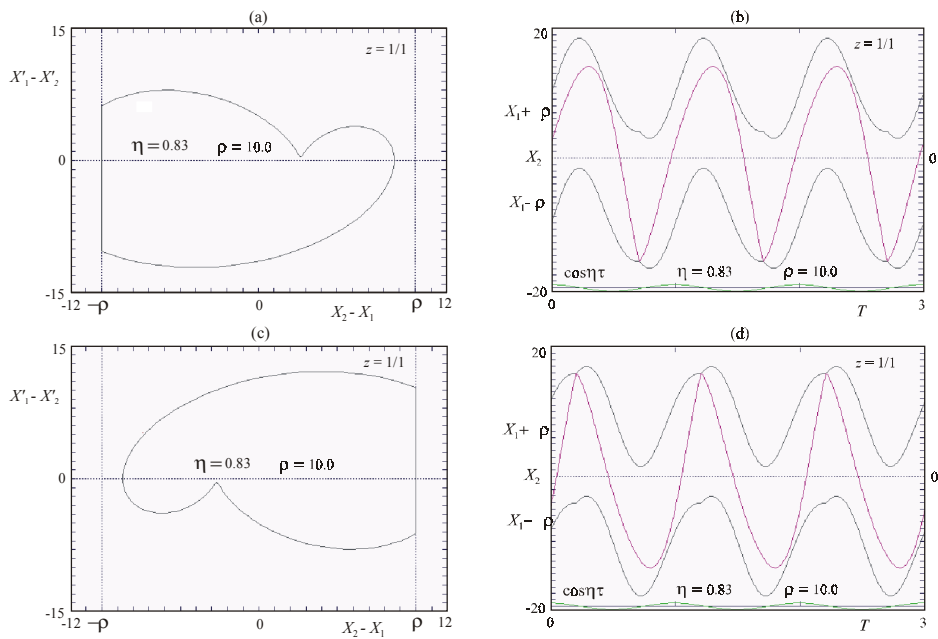


Fig. 6. Mirror regimes of one-impact motion

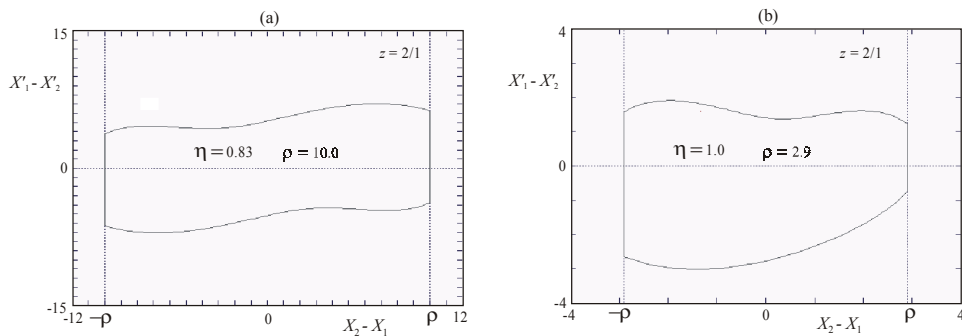


Fig. 7. Symmetric (a) and asymmetric (b) two-impact motion

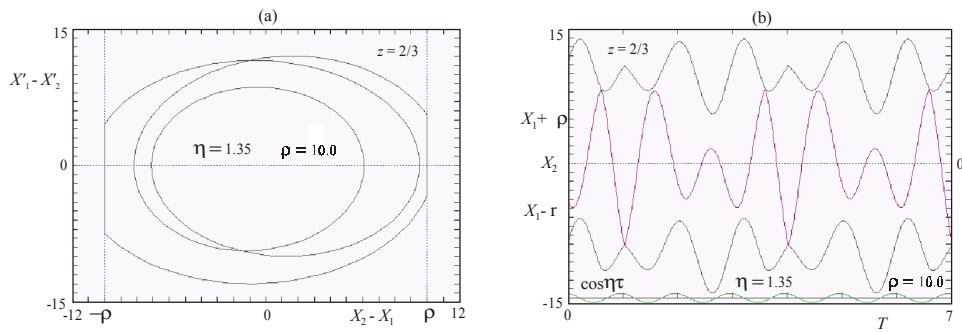


Fig. 8. Subharmonic motion with two impacts per three excitation periods

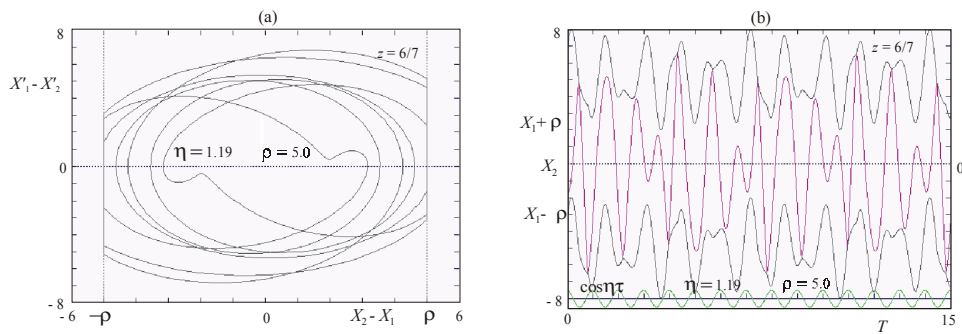


Fig. 9. Subharmonic motion with six impacts per seven excitation periods

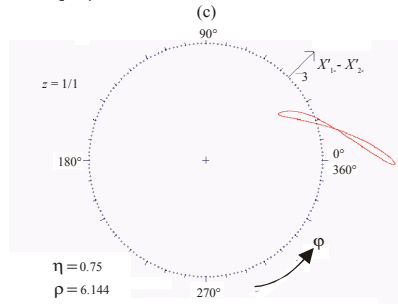
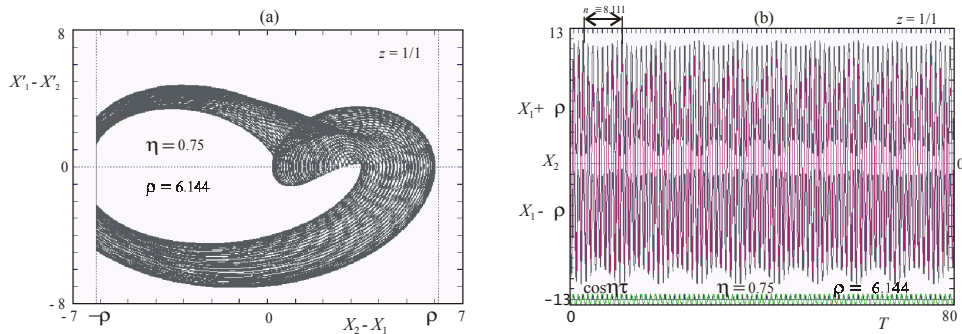


Fig. 10. Quasiperiodic motion with one impact in every excitation period, but motion repeats with quasiperiod $n \cong 8.111$

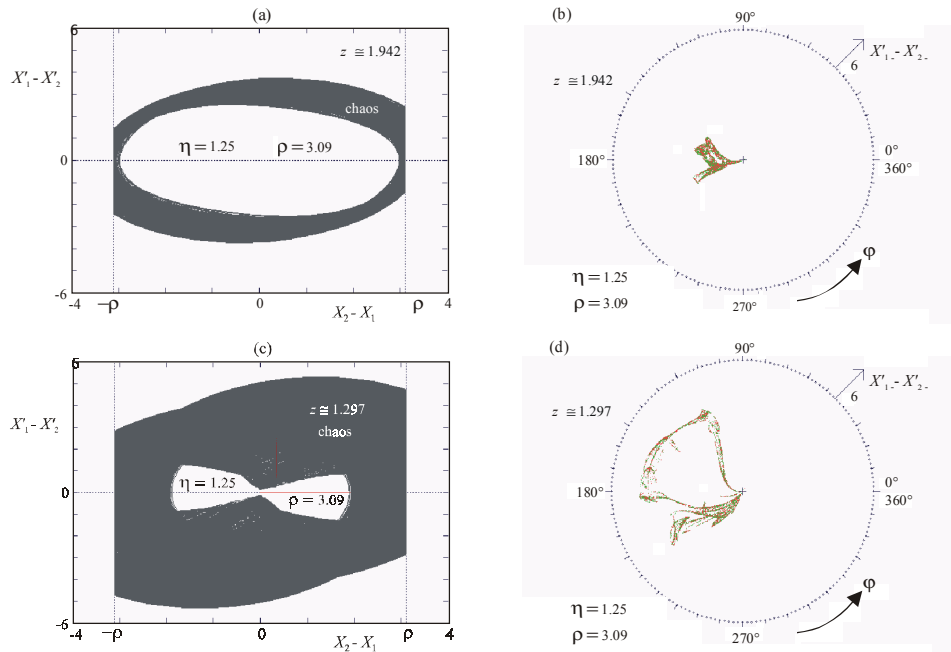


Fig. 11. Two different chaotic regimes (weak (a),(b) and strong (c),(d)) for the same system parameters

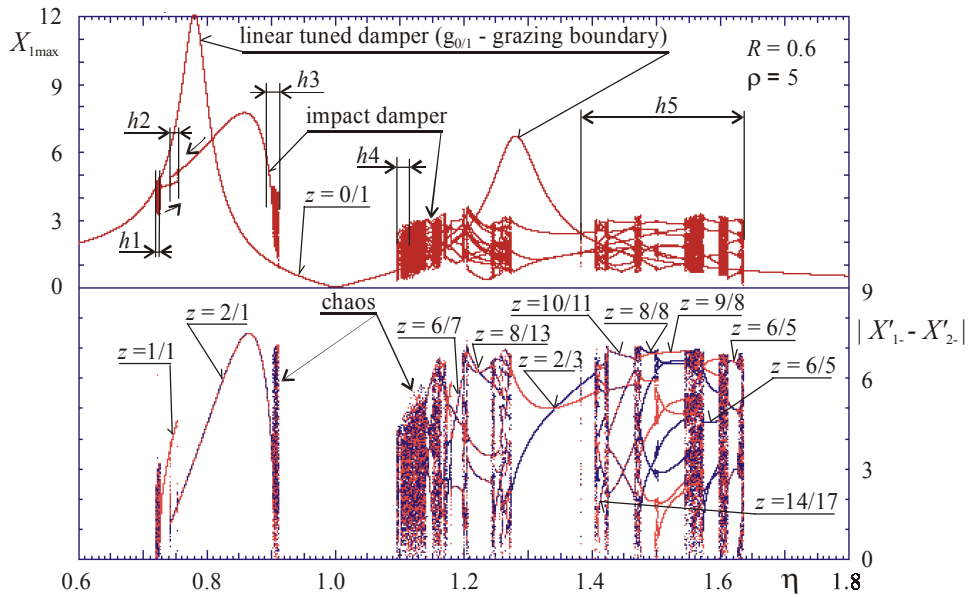


Fig. 12. Bifurcation diagram along line a-a in Fig 4

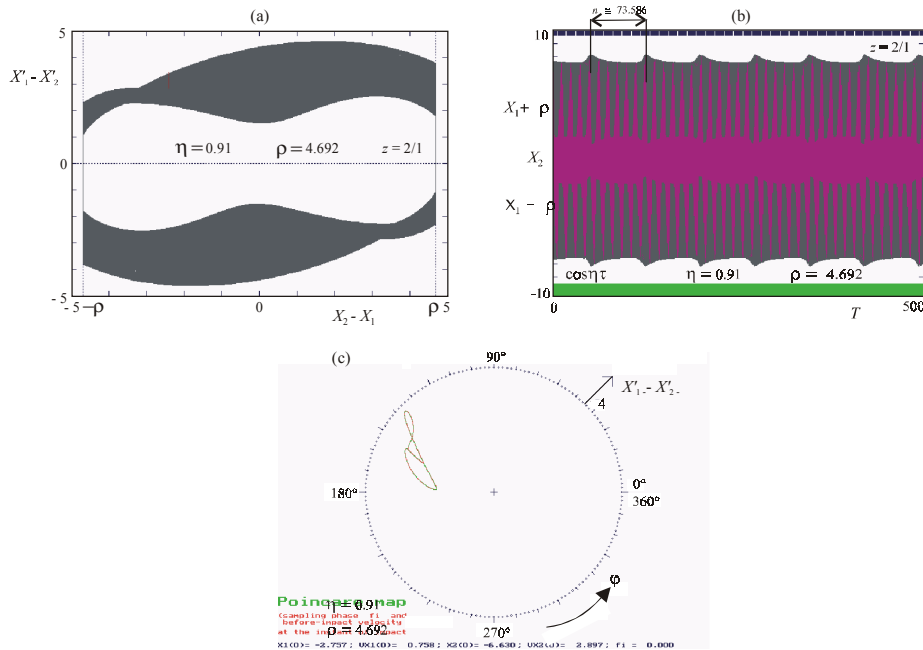


Fig. 13. Quasiperiodic symmetric motion with two impact in every excitation period, but motion repeats with quasiperiod $n \cong 73.586$

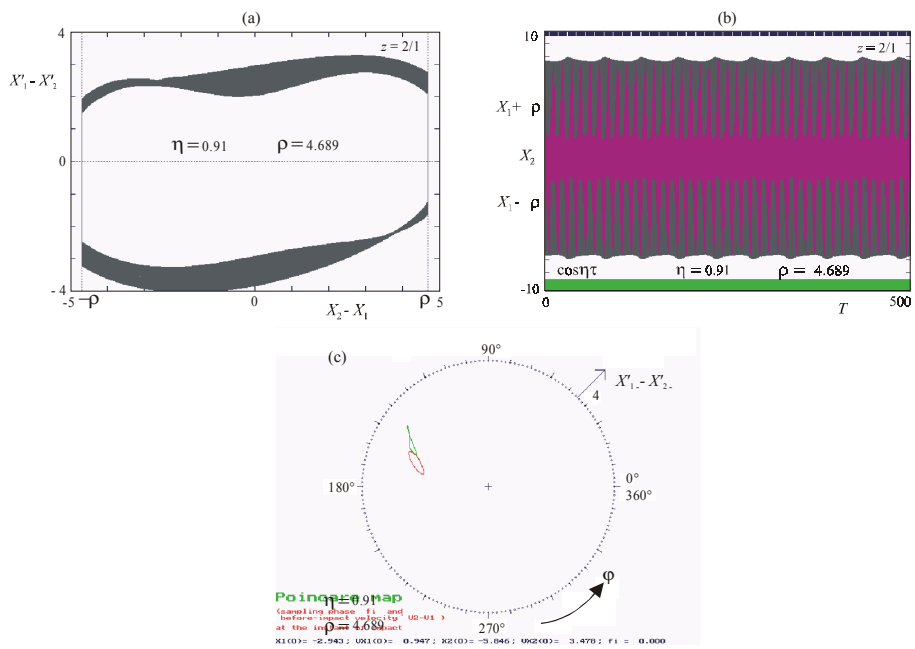


Fig. 14. Quasiperiodic asymmetric motion with two impact in every excitation period, but motion repeats with quasiperiod $n \cong 50.35$

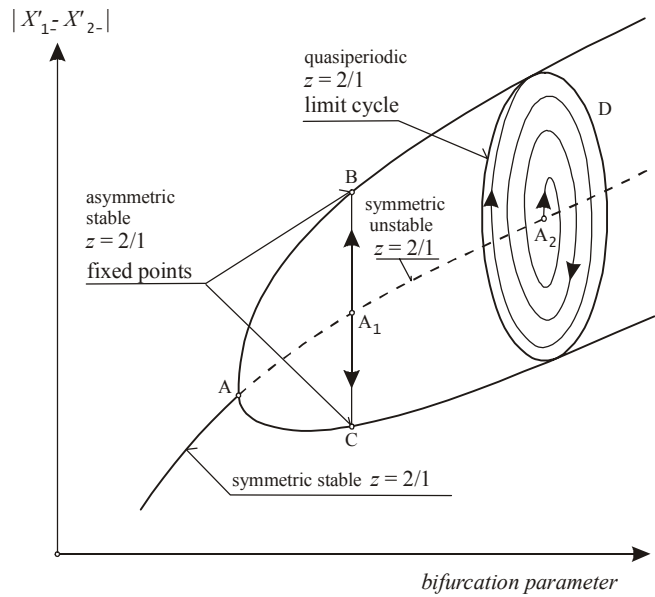


Fig. 15. Scheme of the Hopf bifurcation

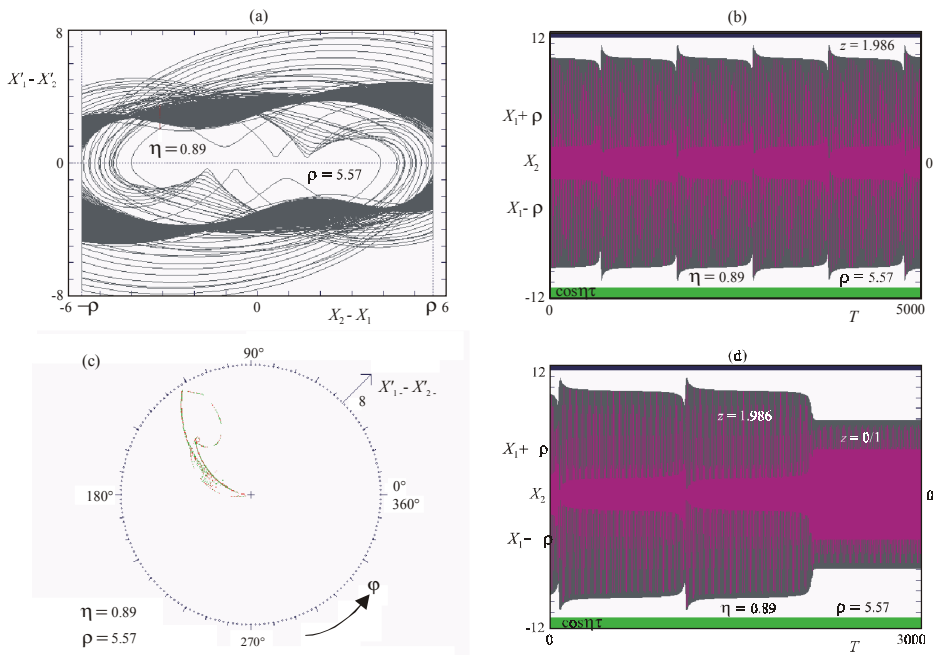


Fig. 16. Intermittency chaos in almost quasiperiodic regime with approx. $n \cong 1023.4 T$ (a),(b),(c); the development of $z=2/1$ impact motion instability is not interrupted and system motion jumps into impactless regime (last part of (d))

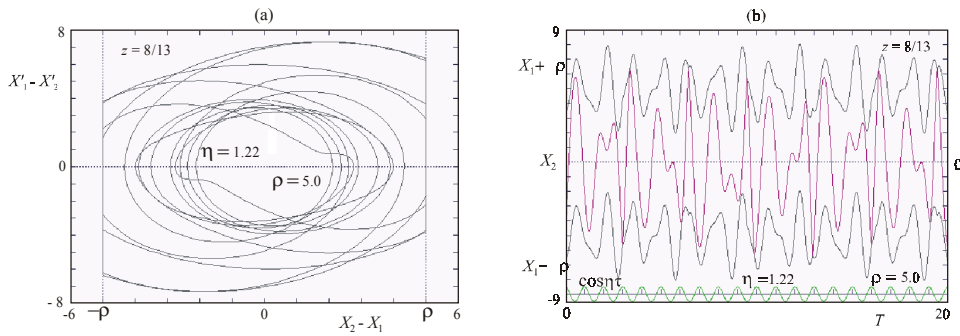


Fig. 17. Symmetric subharmonic motion with 8 impacts per 13 excitation periods T

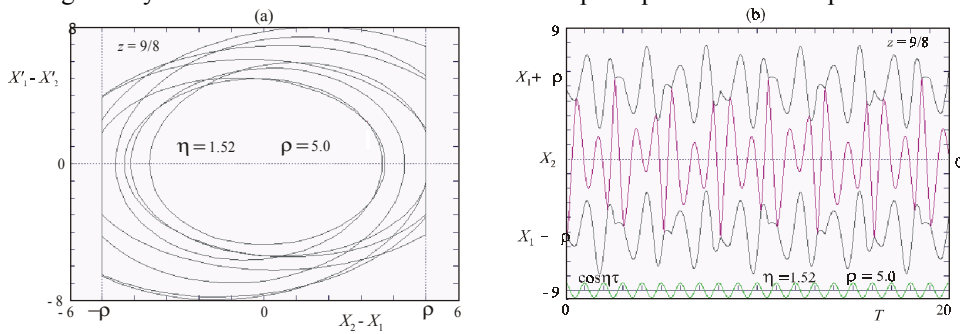


Fig. 18. Asymmetric subharmonic motion with 9 impacts per 8 excitation periods T

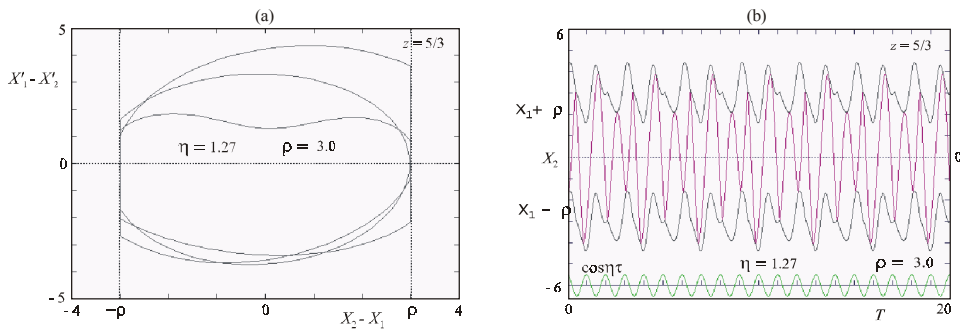


Fig. 19. Asymmetric subharmonic motion with 5 impacts per 3 excitation periods T

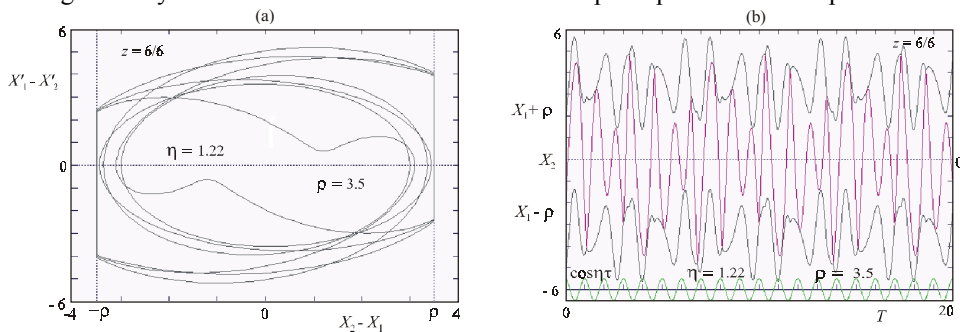


Fig. 20. Symmetric subharmonic motion with 6 impacts per 6 excitation periods T

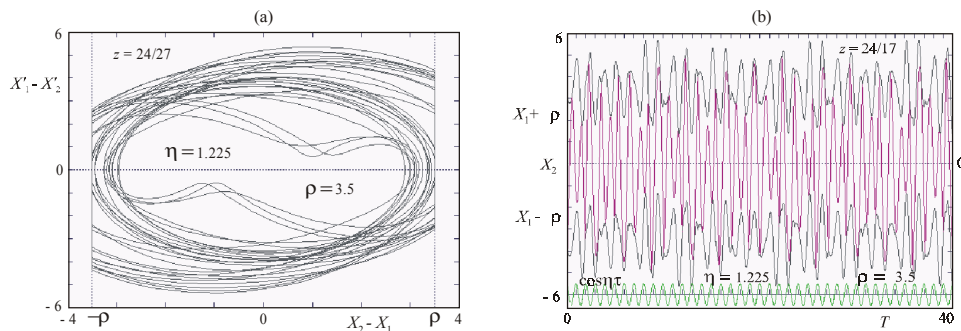


Fig. 21. Symmetric subharmonic motion with 24 impacts per 27 excitation periods T

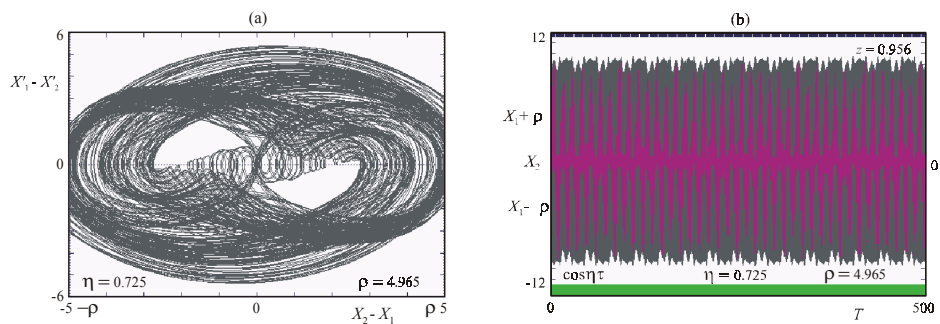


Fig. 22. Symmetric subharmonic motion with 280 impacts per 292 excitation periods T

4.2. Quasiperiodic impact motions

Contrary to impact oscillators with one degree of freedom, where exists the Hopf bifurcation in the form of motion period doubling, the Hopf bifurcation resulting in quasiperiodic motion exists in impact oscillators with two and more degrees of freedom [13]. The substance of this bifurcation was explained by Fig. 15. Examples of quasiperiodic $z=1/1$, $z=2/1$ symmetric and $z=2/1$ asymmetric motions are shown on Figs. 10, 13 and 14, respectively. Quasiperiods of such motions are $n \cong 8.111$, 73.586 and 50.35 , respectively.

4.3 Intermittency chaos

The existence of the intermittency chaos was explained in [14]. It can appear after saddle-node instability of periodic impact motion, when an additional impact interrupts the development of this instability. An example of the intermittency chaos in the impact damper is shown in Figs. 16(a),(b),(c), corresponding to point $P7$ in Fig. 4. This motion seems like the quasiperiodic motion with $n \cong 1023.39 T$, but its substance is the intermittency. During almost whole quasiperiod n develops the saddle-node instability of $z=2/1$ motion (see dark area in Fig.16(a), where approximately two quasiperiods of motion are recorded), at the end of which some of regular two impacts per cycle disappears (mean value of $z \cong 1.986$) and system motion endeavours jump into impactless $z=0/1$ motion, which is shown in Fig. 16(d). In that time an additional impact appears, which takes the system motion back to the state of the beginning of the instability

development. This motion has the chaotic character (see also the attracting set in Poincaré map, Fig. 16 (c)), because the instant and the intensity of additional impact are unpredictable.

4.4 Chaotic and more complex subharmonic impact motions

It follows from bifurcation diagram in Fig. 12, that there exist many periodic subharmonic and chaotic motions in regions of beat motion. Some of them were shown in Figs. 17 - 22 for more detail view on the dynamics of this impact damper. They are lucidly described in Tab. 1. Some of them, e.g. motion in Fig. 22, can be heavily classified, but they can be definitely declared as periodic motions.

Table 1. Characteristics of subharmonic impact motions

| Figure | Point in Fig. 4 | z | Characterisation |
|--------|-----------------|---------|------------------|
| 17 | P8 | 3/8 | symmetric |
| 18 | P9 | 9/8 | asymmetric |
| 19 | P10 | 5/3 | asymmetric |
| 20 | P11 | 6/6 | symmetric |
| 21 | P12 | 24/27 | asymmetric |
| 22 | P13 | 280/292 | symmetric |

5. CONCLUSION

This paper gives the more detail insight on the behavior of the dynamical impact damper. Firstly are evaluated regions of existence and stability of different regimes of its response on harmonic excitation and then impact motions are explained using bifurcation diagrams, time series, phase trajectories and Poincaré maps.

It follows from Fig. 12 and [15], that such system wholly eliminates the main resonance amplitudes of the fundamental vibrating system with one degree of freedom (at frequency $\eta = 1$) owing to the additional of linear tuned damper. The original resonance divides therefore on two resonances, which amplitudes are suppressed, especially in higher resonance, by the possibility of impact interaction between mass of original system and additional mass of the damper.

Acknowledgement. *This investigation was supported by the Pilot Project No. 50 351 of the Institute of Thermomechanics AS CR under the research purpose No. AVOZ 2076919.*

REFERENCES

1. Grubin C., On the theory of the acceleration damper, Trans. of the ASME, Journal of Applied Mechanics, September 1956, pp. 373-378.
2. Arnold R.N., The acceleration absorber, Proceedings of International Conference of Applied Mechanics, 1956, 367-372.
3. Egle D.M., On Investigation of an Impact Vibration Absorber, Trans. of the ASME, Journal of Engineering for Industry, November 1967, pp. 653-661.
4. Masri S.F., Theory of the Dynamic Vibration Neutralizer With Motion-Limiting Stops, Trans. of the ASME, Journal of Applied Mechanics, June 1972, pp. 563-568.

5. Cempel C., Receptance model of the multi-unit vibration impact neutralizer "MUVIN", *J. Sound and Vibration*, 40, 1975, pp. 249-266.
6. Peterka F., An investigation of the Motion of Impact Dampers, Paper I - Theory of the Fundamental Impact Motion, *Strojnícky časopis*, XXI, No. 5, 1970, pp. 457-478, Paper II - Properties of the Motion of Two -Stop-Spring Impact Dampers, *Strojnícky časopis*, XXI, No. 6, 1970, pp. 567-584
7. Peterka F., An investigation of the Motion of Impact Dampers, Paper III - Comparison of the Properties of Motion and Optimization of Parameters of Three Types of Impact Dampers and a Linear Dynamic Damper, *Strojnícky časopis*, XXII, No. 5, 1971, pp. 428-444.
8. Peterka F., Analysis of Motion of the Impact-Dry-Friction Pair of Bodies and its Application to the Investigation of the Impact Dampers Dynamics, *Proc. of MOVIC'99, 17th Biennial Conference on Mechanical Vibration and Noise*, Las Vegas, USA, 1999, 1-10, see also *Proc. "Applied Nonlinear Dynamics and Chaos of Mechanical Systems with Discontinuities"* (Eds. Marian Wiercigroch & Bram de Kraker), World Scientific Series on Nonlinear Science, Series A, Vol. 28, 2000, pp. 343-359.
9. Yoshitake Y., Sueoka A., Quenching of Self-Excited Vibrations by Impact Damper. *Proc. "Applied Nonlinear Dynamics and Chaos of Mechanical Systems with Discontinuities"* (Eds. Marian Wiercigroch & Bram de Kraker), World Scientific Series on Nonlinear Science, Series A, Vol. 28, 2000, pp. 155-176
10. Blazejczyk-Okolewska B., Analysis of an Impact Damper of Vibration. *Chaos, Solitons & Fractals*, 12, 2001, 1983-1988.
11. Čipera S., Černá R., Peterka F., Characteristics of the Motion of Mechanical Impact Systems with Dry friction, *Proc. 2nd European Nonlinear Oscillations Conference*, Prague, Sept. 9-13, 1996, Vol. 1, pp. 129-132.
12. Peterka F., Vibro-Impact Systems. Chapter in Encyclopedia of Vibration, *Academic Press Ltd*, London 2001, Vol. 3, pp. 1531-1548.
13. Peterka F., Vacík, Transition to chaotic motion in mechanical systems with impacts. *Journal of Sound and Vibration* 1992, 154 (1), pp. 95-115.
14. F. Peterka, Dynamics of the Impact Oscillator. Abstracts, IUTAM Chaos'97, Symposium, Cornell University, July 27-August 1, 1997, *Proc. Kluwer Academic Publishers*, Dordrecht, 1998, pp. 283-292.
15. Peterka F., Blazejczyk-Okolewska B., Some Aspects of the Dynamical Behaviour of the Impact Damper. *Journal of Vibration and Control*, Sage Science Press (in print).

DETALJNIJI POGLED U DINAMIKU UDARNIH PRIGUŠIVAČA

František Peterka

Kretanje dinamički uradnog prigušivača je studirano korišćenjem numeričke simulacije. Oblasti postojanja i stabilnosti različitih režima odgovora sistema na harmonijsku pobudu je ocenjivana i vrednovana. Granice oblasti su specifičirane, kao opadanja, udvostručenog perioda, singularne tačke sedlo-čvor i Hopf-ova bifurkacija. Periodička, kvazi-periodička i haotično udarna kretanja su izražena pomoću redova u zavisnosti od vremena, faznih trajektorija, bifurkacionih dijagrama i Poincaré-ovih mapa.